Heavy Gas Dispersion in Presence of Large Obstacles: Selection of Modeling Tools

Marco Derudi, Daniele Bovolenta, Valentina Busini,* and Renato Rota

Department of Chemistry, Materials and Chemical Engineering "G. Natta", Politecnico di Milano, Piazza Leonardo da Vinci 32, Milano, Italy

1. INTRODUCTION

Industrial accidents involving chemical installations and chemical transportation occur with relative frequency and may result in large numbers of fatalities when they involve the release of hazardous gases with density values larger than that of the ambient air (the so-called "heavy" or "dense" gases) because the resulting clouds lay close to the ground for large distances from the release point.

In the last years, attention has been focused in particular on the so-called TICs (toxic industrial chemicals)[1−5] and on the emerging risks related to LNG regasification plants.[6−15] With respect to the former, the large-scale production of TICs and their potential for widespread exposure and significant public health impact makes accidental releases of TICS an important area of concern, while for LNG regasification plants, the main concern is related to the relatively new technologies involved and to the large increase in new installations foreseen for the near future.

The release of TICs or large spills of LNG may occur either inside the production plants or even in an urban context (e.g., in case of accidental release from a rail tank); in both cases, the atmospheric dispersion of the resulting hazardous cloud happens in environments with an intrinsically complex geometry. However, the risk assessment of accidental releases of hazardous gases is still largely performed using integral models, such as DEGADIS, SLAB, ALOHA, and UDM.[16−18] Integral models are lumped-parameter models, usually pseudo-one-dimensional, which account for some physical phenomena using semiempirical relationships whose parameters are tuned on field test data.[19] They are relatively easy to use and do not require large computational resources, but their accuracy depends upon the experimental tests used for tuning the model parameters. Because the experimental setup of these field trials usually does not involve any significant obstacle, these models can provide reliable results only in open field conditions, that is, when almost no obstacles are present in the cloud region.

For simulating the atmospheric dispersion of hazardous gas clouds in geometrically complex environments, mathematical models developed in the frame of computational fluid dynamics (CFD) have to be used. In fact, CFD models perform a fully three-dimensional simulation of the involved geometry, thus accounting for the influence of the environment's geometry on the gas cloud dispersion.[20−23] Clearly, in open field conditions (that is, when no obstacles are present), both integral and CFD models are expected to give similar results, at least when considering situations close to those used for tuning the integral model parameters. This has been shown in a previous work,[24] considering for the sake of example some experimental data involving open field SO_2 releases.[25]

However, the use of CFD models requires a much larger amount of resources, both in terms of time and analyst skill, to perform the cloud dispersion simulations. As a consequence, the use of a CFD model should be restricted to cases where the gas cloud dispersion is significantly influenced by the environment's geometry because using an integral model in geometrically complex environments could lead to significant errors in determination of the hazardous area dimensions, while using a CFD model when simple geometries are involved could lead to a meaningless waste of resources. Given the large number of simulations usually involved in the quantitative risk analysis of an industrial plant, even the last problem plays a fundamental role in guaranteeing reliable results of risk analysis and therefore plant safety. This highlights how important is to evaluate and choose appropriate numerical models and boundary conditions through the understanding of their strengths and possible drawbacks.[23]

Over the past few years, several CFD studies applied to complex environments have been carried out.[3,5,26−36] Most of these studies underly the influence of obstacles on gas dispersion, but none of them delineating a criterion able to

Received: October 16, 2013
Revised: December 19, 2013
Accepted: December 19, 2013
Published: December 19, 2013

foresee when the influence of an obstacle on the dispersion of a dense gas cloud cannot be disregarded. Such a criterion would be important at least for three practical reasons: First, it would permit for deciding a priori when integral models can be safely used in performing a quantitative risk analysis, avoiding the aforementioned problems (large errors using integral models when CFD models should be used or large waste of resources using CFD models when integral models could be used). Second, the same criterion could be used to simplify the representation of the real environment's geometry in the computational domain by considering only the obstacles that are relevant for cloud dispersion, therefore strongly reducing the numerical problems related to the ratio between the smallest computational grid size (required to mesh correctly the smaller geometrical detail considered) and the largest dimension of the integration domain. Third, the criterion would allow for foreseeing at first glance the size of a mitigation wall aimed to reduce the hazardous area arising from the accidental release of a hazardous compound because the dimension of the mitigation wall should be at least equal to that able to influence significantly the dispersion of a dense gas cloud.

Therefore, the main aim of this work is to provide a criterion able to define how large an obstacle should be to influence significantly the dispersion of a cloud of dense gases. Such a criterion was deduced from the results of a large number of heavy gas dispersion simulations carried out with a CFD model in the presence of a wide range of different obstacles.

2. MATERIALS AND METHODS

Among the approaches recently proposed to describe the neutral atmospheric boundary layer in CFD studies,[24,37−39] in the present study, the ASsM method[24] was used to represent the effects of turbulence. The ASsM approach is based on the standard $k-\varepsilon$ model, with the standard Jones and Launder values[40] for the constants, and requires an additional source term in the ε balance equation, S_ε, to ensure consistency between $k-\varepsilon$ model predictions and Monin−Obhukov similarity theory profiles across the integration domain.

Fully developed vertical profiles of velocity, temperature, turbulence intensity, and dissipation rate coherent with the Monin−Obhukov similarity theory were used as boundary conditions at the wind inlet boundary. Standard boundary conditions were used for all the other boundaries. The commercial package Fluent 12[41] was used for all the computations.

3. RESULTS AND DISCUSSION

As previously mentioned, the aim of this work is to develop a general methodology to discriminate between situations where CFD or integral models should be used to assess the consequences of heavy gas dispersions with obstacles on the cloud pattern.

To develop such a methodology, a parametric analysis was performed, using as a target function the difference between the gas cloud size in the open field and in the presence of an obstacle with a given geometry. Steady-state releases of an intrinsic heavy gas with an obstacle located downwind of the release point were considered as a case study; the dense gas was released vertically at 10 m/s from a circular section with a diameter of 0.6 m located on the symmetry plane of the considered domain and 350 m downwind of the wind inlet section. The cloud dispersion was studied over a computational domain of 1500 m × 250 m × 400 m, which represents half of a full 3D symmetric domain with a vertical symmetry plane directed as the wind flow and passing to the center of the gas source.

A standard procedure for mesh generation was used, imposing unstructured triangular elements on both the inlet section and the obstacle; tetrahedral elements were obtained with a vertical growth of the base mesh. A uniform size function was imposed, starting from the meshed surfaces and attached to the whole domain; growth rate was set 1.2 with a maximum cell size of 20 m. The domain was discretized by a tetrahedral unstructured grid with a total mesh size of 800,000 elements. Grid independence of the results was checked by repeating the simulation of a reference case using halved size elements; no significant differences in the target function were found between the two simulations. A typical computational domain realized to perform the parametric study is shown in Figure 1.

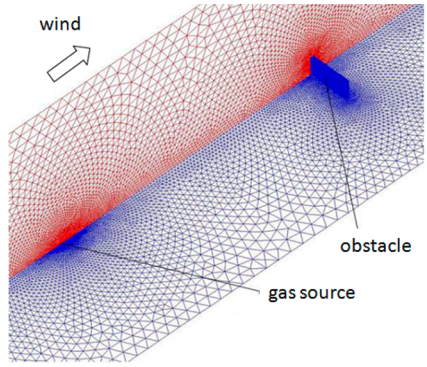

Figure 1. Detail of the computation domain realized for one of the investigated cases.

The boundary conditions used in all the simulations are summarized in Table 1. Frontal, lateral, and upper boundary faces were set as velocity inlet, introducing wind, k, and ε profiles by means of dedicated user-defined functions. The back face was set as a pressure outlet, while the gas inlet was imposed through a velocity inlet on the circular source section. Finally, for the wall surfaces, a roughness value of 0.05 m was used. All the simulations were carried out considering a neutral stratification of the atmosphere with 5 m/s wind at a reference height aboveground of 10 m, which is one of the most common atmospheric conditions used in risk assessment studies.

Table 1. Boundary Conditions Used in All the Simulations

boundary	type
wind inlet	velocity inlet, 300 K
wind outlet	pressure outlet
top boundary	velocity inlet, 300 K
external lateral boundary	velocity inlet, 300 K
internal lateral boundary	symmetry
ground	wall, 300 K; roughness, 0.05 m
gas inlet	during the atmospheric stabilization: wall, 300 K; roughness, 0.05 m
	during the release: velocity inlet, 300 K
walls	wall, roughness, 0.05 m

Table 2. Configurations Investigated in the Parametric Study

case #	ρ_{gas} (kg/m^3)	x_{obs} (m)	h_{obs} (m)	w_{obs} (m)	C_{ref} (ppmv)
1	2.77	open field	0.00	0.00	2000/1000/750/500/250
2−45	2.77	400	2.50	7.50	500/250[a]
			3.75		
			15.00		
			5.00	15.00	
			7.50		
			15.00		
			30.00		
			10.00	30.00	
			15.00		
			30.00		
			60.00		
			20.00	60.00	
			30.00		
			60.00		
			120.00		
			15.00	45.00	
			22.50		
			45.00		
			90.00		
			45.00	90.00	
			60.00	120.00	
			75.00	150.00	
46−60	5.44	400	7.50	15.00	750/500/250[a]
			15.00	30.00	
			30.00	60.00	
			45.00	90.00	
			75.00	150.00	
61−80	8.31	400	7.50	15.00	1000/750/500/250[a]
			15.00	30.00	
			30.00	60.00	
			45.00	90.00	
			75.00	150.00	
81−100	2.77	150	7.50	15.00	2000/1000/750/500/250
			15.00	30.00	
			30.00	60.00	
			45.00	90.00	
101−120	5.44	150	7.50	15.00	2000/1000/750/500/250
			15.00	30.00	
			30.00	60.00	
			45.00	90.00	
121−140	8.31	150	7.50	15.00	2000/1000/750/500/250
			15.00	30.00	
			30.00	60.00	
			45.00	90.00	
141−216	2.77	250	2.50	4.50	1000/750/500/250[a]
			3.75		
			15.00		
			5.00	9.00	
			7.00		
			7.50		
			30.00		
			10.00	18.00	
			14.00		
			15.00		
			60.00		
			15.00	27.00	
			22.50		
			90.00		
			20.00	36.00	
			28.00		

Table 2. continued

case #	ρ_{gas} (kg/m^3)	x_{obs} (m)	h_{obs} (m)	w_{obs} (m)	C_{ref} (ppmv)
			30.00		
			120.00		
			42.00	54.00	
217–242	2.77	85	3.50	4.50	2000/1000/750/500/250
			7.00	9.00	
			14.00	18.00	
			28.00	36.00	
			42.00	54.00	

[a]Only threshold concentrations at which there is a significant interaction between the obstacle and the gas cloud have been evaluated.

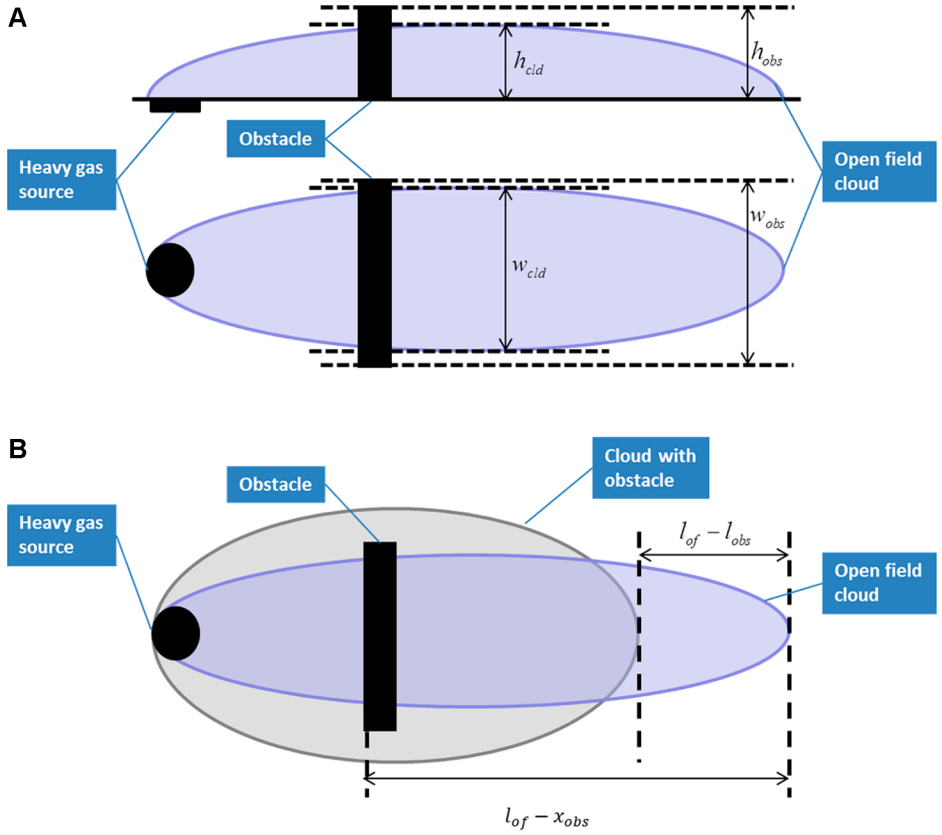

Figure 2. Schematic representation of the interaction between gas cloud and obstacle. (A) Vertical section (upper part) and footprint (lower part) of the cloud in open field conditions together with the vertical (upper part) and horizontal (lower part) view of the obstacle. The main characteristic dimensions of both the obstacle and the cloud in open field conditions are identified. (B) Footprint of the cloud both in open field conditions and in the presence of the obstacle. The target function representing the effect of the obstacle on the cloud size is identified.

The parameters whose influence was investigated in the sensitivity analysis are obstacles geometry (except for the thickness, which was equal to 5 m for all the obstacles; this value from one side does not affect significantly the results and on the other side does not require thickening strongly the mesh close to the wall); obstacle downwind distances from the release source (x_{obs}); gas density; and cloud dimensions, varied by changing the threshold concentration value (C_{ref}). The full set of the investigated cases (nearly 250 cases, with an aspect ratio, defined as the ratio between the two relevant dimensions of the obstacle, ranging from 0.3 to 3.0) is summarized in Table 2.

To synthesize the characteristics of the different parameters investigated, which are relevant for the sensitivity analysis carried out, a simple dimensionless parameter comparing the characteristic dimensions of the cloud and the obstacle was used. Considering an obstacle completely embedded in the cloud, two characteristic dimensions of the obstacle are expected to play a role in modifying the cloud size, namely, the obstacle height, h_{obs}, and the obstacle width, w_{obs}. Such characteristic dimensions of the obstacles should be compared with the respective characteristic dimensions of the cloud in open field, that is, the cloud height, h_{cld}, and the cloud width, w_{cld}, as shown in Figure 2. The ratios between the corresponding characteristic dimensions of the obstacle and the cloud can be defined as dimensionless parameters whose values represent the relative importance of the obstacle size to the cloud size in the horizontal and lateral direction, respectively

$$R_h = \frac{h_{obs}}{h_{cld}} \quad (1)$$

$$R_w = \frac{w_{obs}}{w_{cld}} \quad (2)$$

It should be noted that the cloud dimension refers to a given gas concentration. Therefore, the R_h and R_w values change with the chosen concentration of interest. Moreover, because R_h and R_w have generally different values, a global parameter, accounting for the relative cloud/obstacle ratio in both the directions, should be defined. This definition can arise from the observation that a very tall and thin (with respect to the cloud size) obstacle has an almost negligible influence on the cloud size because the cloud can easily turn around it without raising in the vertical direction; conversely, a very large but low (with respect to the cloud size) obstacle can be stepped over with negligible lateral spreading of the dense gas cloud. Therefore, the smaller value of the parameters R_h and R_w is expected to determine whether an obstacle plays a major role or not, leading to the following definition of the overall parameter, R^*

$$R^* = \min(R_h, R_w) \quad (3)$$

Situations characterized by small values of R^* are expected to behave similarly to open fields releases, while when the value of R^* is large the cloud behavior with obstacles present is expected to be quite different from the cloud behavior in open field conditions.

The target function used to synthesize the change in cloud behavior due to the presence of an obstacle is related to the variation of the cloud length from the obstacle position, as shown in Figure 2. This choice reflects the assumption that only situations where the cloud in open field reaches the obstacle location were considered in this work. In particular, the dimensionless relative change in the cloud length from the obstacle position, Δ, was used

$$\Delta = \frac{l_{of} - l_{obs}}{l_{of} - x_{obs}} \quad (4)$$

where l_{of} is the maximum downwind length reached by the cloud in open field, and l_{obs} the maximum length reached by the cloud when the obstacle is present. Δ is positive when the obstacle reduces the cloud length, while it is negative when the cloud length is enhanced by the presence of the obstacle.

From a qualitative analysis of the interaction between the gas cloud and the obstacle carried out for different cases, several characteristic cloud behaviors can be identified, as shown for the sake of example in Figure 3, where the same source term, both in terms of mass flow rate and position, was considered; only the wall dimensions were varied in the four situations shown in the figure while keeping the same downwind position. For low R^* values, two main behaviors were observed, which were that very large and low obstacles have a small and sometimes negative influence on the gas plume dispersion. Actually, the gas dilution can be reduced in the region close to the upwind face of the obstacle, where wind speed is almost zero, and then the obstacle itself can act as a kind of launching pad for the gas cloud, slightly increasing the maximum distance reached by the cloud in comparison with the open field gas cloud behavior (Figure 3A). When very small obstacles (with respect to the cloud size) are involved, the obstacle produces small variations in the cloud maximum distance (Figure 3B). Therefore, in order to ensure a significant effect of the obstacle on the gas cloud behavior, both the characteristic obstacle dimensions have to be increased, thus increasing the R^* value as shown in Figure 3C. Finally, very large and tall obstacles,

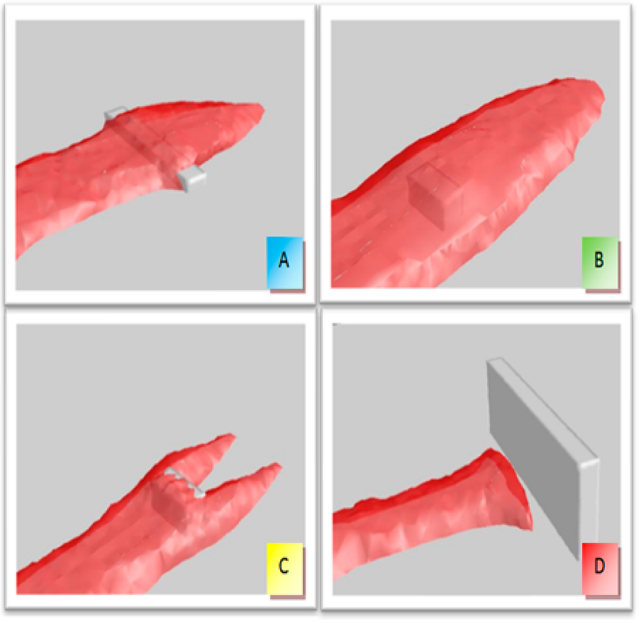

Figure 3. Typical interactions between gas cloud and obstacle. In all cases, the same source term, both in terms of mass flow rate and location, was considered, and only the wall dimensions were varied at a constant downwind position. (A) Large and low obstacles are not able to stop the cloud. They can either have a small influence on the gas plume dispersion or behave like a launch pad. (B) Very small obstacles are involved. The obstacle produces small variations in the cloud maximum distance. (C) The wall is high enough but not large enough to stop the cloud. (D) The wall acts as a mitigation barrier and stops the cloud.

characterized by high R^* values, produce a sort of "barrier effect", producing a strong variation in the cloud behavior (Figure 3D).

The sensitivity of the cloud behavior with respect to all the parameters investigated can be summarized using the aforementioned target function, Δ, and overall parameter, R^*. We can see that the general trend is coherent because the value of Δ increases with R^* as shown in Figure 4. Moreover, the Δ values are generally positive; this means a reduction in the cloud maximum length when the obstacle is present. Only for small values of the parameter R^* are negative Δ values observed, meaning that these obstacles, as previously mentioned, can raise the cloud slightly and consequently can increase its maximum downwind length with respect to open

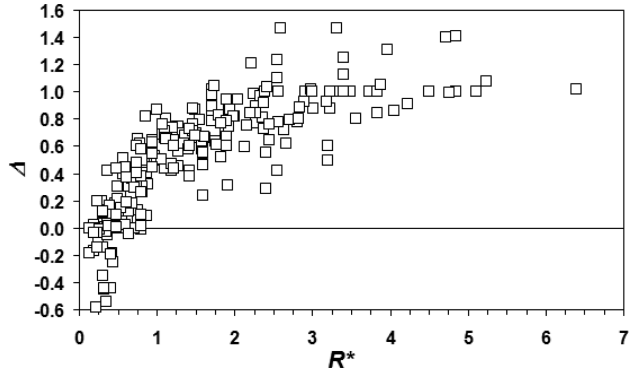

Figure 4. Effect of the obstacle on a dense gas cloud dispersion expressed in a Δ vs R^* plot.

field conditions (Figure 3A). For the sake of generality, all the data summarized in Figure 4 have been obtained using CFD simulations to evaluate the hazardous distances both in open field conditions and in the presence of the wall. However, similar results can be obtained using an integral model to estimate the gas cloud size in open field conditions (that is, without the presence of obstacles), provided that the intrinsic limitations of the integral model allows its use for simulating the considered release scenario. This has been confirmed for the data reported in Figure 4 using the ALOHA integral model when the chemical species were included in the ALOHA database.

From the data reported in Figure 4, three regions can be identified where the sensitivity of the cloud behavior to the presence of an obstacle changes significantly, as shown in Figure 5.

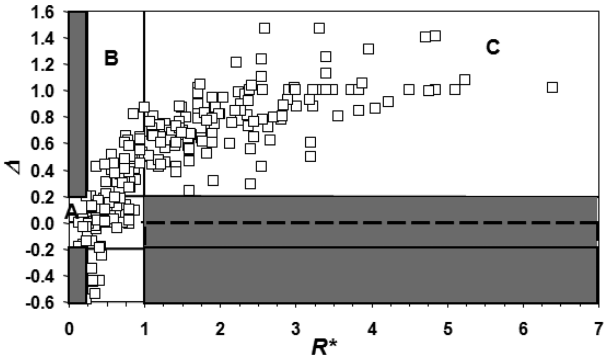

Figure 5. Classification of different regions that highlight the effect of the obstacle on a dense gas cloud dispersion.

The first region, labeled "A" in Figure 5, is characterized by values of R^* lower than 0.25 (that is, the cloud size is four times wider and/or higher than the obstacle), where all the Δ values lie in the range from -0.2 to 0.2. This means that the presence of the obstacle can induce a (positive or negative) change of the cloud length lower than $\pm 20\%$, that is, quite negligible in comparison with the uncertainties in the estimations of the hazardous distances.

The second region, labeled "C" in Figure 5, is characterized by values of R^* larger than 1 (that is, the obstacle is larger than the cloud size), where all the Δ values are larger than 0.2. This means that the presence of the obstacle always induces a reduction of the cloud length larger than 20%, which can be considered not negligible.

These two regions are connected by a sort of transition region, labeled "B" in Figure 5, where both negligible (that is, lower than $\pm 20\%$) and not negligible (that is, larger than $\pm 20\%$) changes in the maximum cloud length can be induced by the presence of an obstacle in the cloud pattern.

The gray areas in Figure 5 are not allowable regions. Two of them would be representative of small obstacles with respect to cloud size ($0 < R^* < 0.25$) and large variation in the cloud dimensions ($\Delta > 20\%$ in absolute values), and the other one is representaive of large obstacles with respect to cloud size ($R^* > 1$) and small variations in the cloud dimensions ($\Delta < 20\%$ in absolute values).

These results, which cannot be rationalized in terms of either R_h or R_w because the situations where one or the other parameter controls are randomly distributed on the diagram, lead to a simple screening methodology to decide a priori when integral models can be safely used in performing a quantitative risk analysis. Region A in Figure 5 is representative of small obstacles (with respect to the cloud size) that produce small variations of the gas cloud length with respect to the open field situation (where integral models are expected to be reliable, at least in situations not too different from those used to tune their parameters); therefore, a dense gas dispersion scenario characterized by $R^* < 0.25$ can be safely simulated through integral models with an expected error on the hazardous distance estimation not larger than 20%. Conversely, region C in Figure 5 is representative of large obstacles (with respect to the cloud size) associated with large cloud length variations with respect to the open field situation; an accidental scenario represented by $R^* > 1$ strictly requires CFD simulations in order to obtain reliable predictions of the hazardous distances. Finally, Zone B is characterized by intermediate values of R^*, where the qualitative effect of the obstacle cannot be predicted, and consequently, the use of CFD simulations is conservatively suggested.

Thus, summarizing, the following step-by-step procedure is proposed to discriminate when an integral or a CFD model should be used: (1) Compare the characteristics of the accidental release of interest with the intrinsic limitations of the chosen integral model (apart from those related to the presence of obstacles), which are strongly related to the experimental window used for tuning the adjustable parameters of the integral model itself. This should be always the first step because if the more relevant characteristics of the considered release scenario (apart from those related to the presence of obstacles) cannot be reasonably reproduced by the integral model, a CFD approach is required. (2) If the integral model can be used to reproduce the accidental scenario in open field conditions (that is, without the presence of obstacles), then estimatation of the gas cloud size using such an integral model can occur (obviously, also a more reliable CFD model can be used to estimated such a size). The size of the cloud is that related to the concentration value of interest (e.g., IDLH or LFL). (3) Evaluate the characteristic geometrical parameter R^* through eqs 1 -3 for all the relevant obstacles fully embedded in the cloud. If all the values of R^* are lower than 0.25, an integral model can be safely used, otherwise a CFD approach is required.

Moreover, the same criterion can be used to simplify the representation of the real environment's geometry in the CFD computational domain because obstacles characterized by values of $R^* < 0.25$ can be neglected without compromising the simulation reliability. In particular, also for this purpose, the size of the cloud in open field conditions can be obtained using an integral model if it can be used to reproduce the accidental release without the presence of obstacles. However, because in this case a CFD model will be used in any case, a better choice is to carry out a more reliable CFD simulation of the cloud dispersion without the presence of obstacles for estimating the size of the cloud in open field conditions. Therefore, the real CFD simulation domain can be designed by neglecting all the obstacles fully embedded in the cloud while having a R^* value lower than 0.25.

Finally, the proposed criterion also allows the definition of the minimum size of a mitigation wall, which should be characterized by a value of $R^* > 1$ to induce a significant change in the cloud length. Operatively, the size of the cloud without the presence of the mitigation barrier should be obtained from a CFD simulation because as in the previous case, a CFD

model will be used in any case for designing the mitigation wall. Moreover, the presence of large obstacles in an industrial plant usually prevents the use of integral models. Once the size of the cloud without the presence of the mitigation barrier is computed, the position and size of the mitigation barrier can be defined by fulfilling the criterion $R^*>1$.

As a further validation of the proposed methodology, some literature data were reprocessed on the proposed Δ vs R^* plot. The first set of data considered refers to a realistic case study involving a large release of LNG in a typical regasification plant.[6] In this case, the hazardous concentration value considered is relative to the flammable properties of natural gas and therefore equal to the LFL/2 value. This paper reports the hazardous distances for the dispersion of a large spill of LNG in the plant both without the presence of the mitigation barrier and with the presence of several wide mitigation barriers (w_{obs} = 350 m) with different heights (h_{obs} = 3−12 m) through CFD simulations. From the data reported in the paper, the effects of such mitigation barriers are reported on the proposed Δ vs R^* plot as shown in Figure 6 (full symbols). We can see

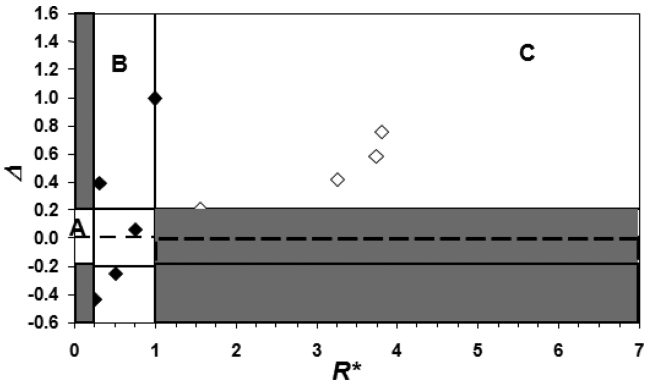

Figure 6. Results obtained applying the proposed methodology to various literature case studies involving a large LNG release in a regasification plant[6] (full symbols) and an ammonia release from a water/ammonia pool[42] (empty symbols).

that in spite of the complex environment considered in this case study (apart from the mitigation barrier, several other large obstacles such as LNG tanks and various equipment have been considered) and the much larger threshold concentration value considered, the methodology proposed in the present work is able to correctly determine the effect of the downwind wall on the gas cloud behavior because all the data lie in the allowable regions as previously defined. As previously mentioned, in this case, using an integral model would not be meaningful because the situation without the large mitigation barrier involves several large obstacles (namely, the regasification plant units and tanks).

The second set of data considered refers to an ammonia release from an aqueous ammonia pool.[42] In this case, the threshold concentration value considered in the CFD simulations is relative to the toxic properties of ammonia and therefore equal to the IDHL value. The authors evaluated the effect of the presence of a large obstacle downwind of the pool (w_{obs} = 48 m, h_{obs} = 12 m) for different wind velocities. From the data reported in the paper, the effects of such an obstacle with various wind speeds are reported on the proposed Δ vs R^* plot as shown in Figure 6 (empty symbols). We can see that also in this case the methodology proposed in the present work is able to correctly determine the effect of the downwind obstacle on the gas cloud behavior because all the data lie in the allowable regions as previously defined. In this case, no other significant obstacles are involved; therefore, the hazardous distance in open field conditions can be computed using an integral model. Also, in this case, no significant deviations between the CFD and ALOHA predictions in open field conditions have been evidenced, which would lead the data computed with CFD and ALOHA results to be almost superimposed in Figure 6.

4. CONCLUSIONS

In this paper, a general criterion to foresee whether the presence of an obstacle on the cloud pattern can influence significantly the hazardous distance resulting from a heavy gas dispersion was proposed. This criterion requires comparing the characteristic dimensions of the obstacles with those of the cloud estimated in open field conditions on a Δ vs R^* plot, with Δ and R^* being two suitable dimensionless parameters.

It was found that when $R^* < 0.25$, the presence of the obstacle can be disregarded. This means that the cloud dispersion can be safely simulated using an integral model, at least when the considered accidental scenario is not too different from those used to tune the parameters of the integral model itself. On the other hand, this also means that the obstacle can be safely neglected when representing the real environment's geometry in the CFD computational domain without compromising the simulation reliability. Moreover, it follows that mitigation barriers characterized by $R^* < 0.25$ cannot perform properly because they cannot induce a significant change in the cloud length.

However, when $R^* > 1$, the presence of the obstacle cannot be disregarded. This means that the cloud dispersion cannot be safely simulated using an integral model and that the obstacle cannot be safely neglected when representing the real environment's geometry in the computational domain. Moreover, mitigation barriers characterized by $R^* > 1$ can perform properly because they induce a significant change in the cloud length.

The proposed methodology was also validated using literature case studies that involve large LNG releases in a regasification plant and ammonia evaporation from an aqueous ammonia pool. In all cases, the proposed methodology was able to foresee correctly the literature findings.

AUTHOR INFORMATION

Corresponding Author

*E-mail: valentina.busini@polimi.it.

Notes

The authors declare no competing financial interest.

REFERENCES

(1) Heinälä, M.; Gundert-Remy, U.; Wood, M. H.; Ruijten, M.; Bos, P. M. J.; Zitting, A.; Bull, S.; Russell, D.; Nielsen, E.; Cassel, G.; Leffler, P.; Tissot, S.; Vincent, J.-M.; Santonen, T. Survey on methodologies in the risk assessment of chemical exposures in emergency response situations in Europe. *J. Hazard. Mater.* **2013**, *244−245* (0), 545.

(2) Sanchez, E. Y.; Colman Lerner, J. E.; Porta, A.; Jacovkis, P. M. Accidental release of chlorine in Chicago: Coupling of an exposure model with a computational fluid dynamics model. *Atmos. Environ.* **2013**, *64* (0), 47.

(3) Hanna, S. R.; Hansen, O. R.; Ichard, M.; Strimaitis, D. CFD model simulation of dispersion from chlorine railcar releases in industrial and urban areas. *Atmos. Environ.* **2009**, *43* (2), 262.
(4) Hanna, S. R.; Chang, J. C.; Zhang, X. M. J. Modeling accidental releases to the atmosphere of a dense reactive chemical (uranium hexafluoride). *Atmos. Environ.* **1997**, *31* (6), 901.
(5) Pontiggia, M.; Derudi, M.; Alba, M.; Scaioni, M.; Rota, R. Hazardous gas releases in urban areas: Assessment of consequences through CFD modelling. *J. Hazard. Mater.* **2010**, *176* (1−3), 589.
(6) Busini, V.; Lino, M.; Rota, R. Influence of large obstacles and mitigation barriers on heavy gas cloud dispersion: a liquefied natural gas case study. *Ind. Eng. Chem. Res.* **2012**, *51* (22), 7643.
(7) Gavelli, F.; Bullister, E.; Kytomaa, H. Application of CFD (Fluent) to LNG spills into geometrically complex environments. *J. Hazard. Mater.* **2008**, *159* (1), 158.
(8) Gavelli, F.; Chernovsky, M. K.; Bullister, E.; Kytomaa, H. K. Modeling of LNG spills into trenches. *J. Hazard. Mater.* **2010**, *180* (1−3), 332.
(9) Hightower, M.; Gritzo, L.; Luketa-Hanlin, A. Safety implications of a large LNG tanker spill over water. *Process Saf. Prog.* **2005**, *24* (3), 168.
(10) Ivings, M. J.; Jagger, S. F.; Lea, C. J.; Weber, D. M. *Evaluating Vapor Dispersion Models for Safety Analysis of LNG Facilities*; HSL (Health and Safety Laboratories): Harpur Hill, Buxton, U.K., 2007.
(11) Koopman, R. P.; Ermak, D. L. Lessons learned from LNG safety research. *J. Hazard. Mater.* **2007**, *140* (3), 412.
(12) Luketa-Hanlin, A. A review of large-scale LNG spills: Experiments and modeling. *J. Hazard. Mater.* **2006**, *132* (2−3), 119.
(13) Luketa-Hanlin, A.; Koopman, R. P.; Ermak, D. L. On the application of computational fluid dynamics codes for liquefied natural gas dispersion. *J. Hazard. Mater.* **2007**, *140* (3), 504.
(14) Pitblado, R. M.; Woodward, J. L. Highlights of LNG risk technology. *J. Loss Prev. Process Ind.* **2011**, *24* (6), 827.
(15) Woodward, J. L.; Pitblado, R. M. *LNG Risk-Based Safety: Modeling and Consequence Analysis*; John Wiley and Sons, Inc: Hoboken, NJ, 2010; p 374.
(16) Bernatik, A.; Libisova, M. Loss prevention in heavy industry: Risk assessment of large gasholders. *J. Loss Prev. Process Ind.* **2004**, *17* (4), 271.
(17) Brook, D. R.; Felton, N. V.; Clem, C. M.; Strickland, D. C. H.; Griffiths, I. H.; Kingdon, R. D. Validation of the urban dispersion model (UDM). *Int. J. Environ. Pollut.* **2003**, *20* (1−6), 11.
(18) Pandya, N.; Gabas, N.; Marsden, E. Sensitivity analysis of Phast's atmospheric dispersion model for three toxic materials (nitric oxide, ammonia, chlorine). *J. Loss Prev. Process Ind.* **2012**, *25* (1), 20.
(19) Hanna, S. R. Hazardous gas-model evaluations: Is an equitable comparison possible? *J. Loss Prev. Process Ind.* **1994**, *7* (2), 133.
(20) Tauseef, S. M.; Rashtchian, D.; Abbasi, S. A. CFD-based simulation of dense gas dispersion in presence of obstacles. *J. Loss Prev. Process Ind.* **2011**, *24* (4), 371.
(21) Steffens, J. T.; Heist, D. K.; Perry, S. G.; Zhang, K. M. Modeling the effects of a solid barrier on pollutant dispersion under various atmospheric stability conditions. *Atmos. Environ.* **2013**, *69*, 76.
(22) Ai, Z. T.; Mak, C. M. CFD simulation of flow and dispersion around an isolated building: effect of inhomogeneous ABL and near-wall treatment. *Atmos. Environ.* **2013**, *77*, 568.
(23) Tominaga, Y.; Stathopoulos, T. CFD simulation of near-field pollutant dispersion in the urban environment: a review of current modeling techniques. *Atmos. Environ.* **2013**, 79.
(24) Pontiggia, M.; Derudi, M.; Busini, V.; Rota, R. Hazardous gas dispersion: A CFD model accounting for atmospheric stability classes. *J. Hazard. Mater.* **2009**, *171* (1−3), 739.
(25) Barad, M. L. *Project Prairie Grass: A Field Program in Diffusion*; Geophysical Research Papers, Project 7657; Air Force Cambridge Research Center, 1958; p 59.
(26) Hanna, S. R.; Tehranian, S.; Carissimo, B.; Macdonald, R. W.; Lohner, R. Comparisons of model simulations with observations of mean flow and turbulence within simple obstacle arrays. *Atmos. Environ.* **2002**, *36* (32), 5067.
(27) Dawson, P.; Stock, D. E.; Lamb, B. The numerical simulation of airflow and dispersion in three-dimensional atmospheric recirculation zones. *J. Appl. Meteorol.* **1991**, *30* (7), 1005.
(28) Letellier, B.; Restrepo, L.; Shaffer, C. J. *Near-Field Dispersion of Fission Products in Complex Terrain Using a 3-D Turbulent Fluid-Flow Model*; 11th Joint Conference on the Applications of Air Pollution Meteorology with the A&WMA, AMS, Boston , MA, 2000; pp 381.
(29) Calhoun, R.; Chan, S.; Leone, R. L.; Shinn, J.; Stevens, D. *Flow Patterns around a Complex Building*; 11th Joint Conference on the Applications of Air Pollution Meteorology with the A&WMA, AMS, Boston, MA, 2000; pp 47.
(30) Kastner-Klein, P.; Plate, E. J. Wind-tunnel study of concentration fields in street canyons. *Atmos. Environ.* **1999**, *33* (24−25), 3973.
(31) DeCroix, D. S.; Smith, W. S.; Streit, G. E.; Brown, M. J. *Large Eddy and Gaussian Simulations of Downwind Dispersion from Large Building HVAC Exhaust*; 11th Joint Conference on the Applications of Air Pollution Meteorology with the A&WMA, AMS, Boston. MA, 2000; pp 53.
(32) Hanna, S. R.; Britter, R.; Franzese, P. A baseline urban dispersion model evaluated with Salt Lake City and Los Angeles tracer data. *Atmos. Environ.* **2003**, *37* (36), 5069.
(33) Hanna, S. R.; Brown, M. J.; Camell, F. E.; Chan, S. T.; Coirier, W. J.; Hansen, O. R.; Huber, A. H.; Kim, S.; Reynolds, R. M. Detailed simulations of atmospheric flow and dispersion in downtown Manhattan: An application of five computational fluid dynamics models. *Bull. Am. Meteorol. Soc.* **2006**, *87* (12), 1713.
(34) Pontiggia, M.; Landucci, G.; Busini, V.; Derudi, M.; Alba, M.; Scaioni, M.; Bonvicini, S.; Cozzani, V.; Rota, R. CFD model simulation of LPG dispersion in urban areas. *Atmos. Environ.* **2011**, *45*, 3913.
(35) Busini, V.; Pontiggia, M.; Derudi, M.; Landucci, G.; Cozzani, V.; Rota, R. Safety of LPG rail transportation. *Chem. Eng. Trans.* **2011**, *24*, 1321.
(36) Labovský, J.; Jelemenský, L. CFD-based atmospheric dispersion modelling in real urban environments. *Chem. Pap.* **2013**, *67*, 1495.
(37) Santos, J. M.; Reis, N. C.; Goulart, E. V.; Mavroidis, I. Numerical simulation of flow and dispersion around an isolated cubical building: The effect of the atmospheric stratification. *Atmos. Environ.* **2009**, *43* (34), 5484.
(38) Parente, A.; Gorle, C.; van Beeck, J.; Benocci, C. A comprehensive modelling approach for the neutral atmospheric boundary layer: Consistent inflow conditions, wall function and turbulence model. *Boundary-Layer Meteorol.* **2011**, *140* (3), 411.
(39) Parente, A.; Gorle, C.; van Beeck, J.; Benocci, C. Improved kappa-epsilon model and wall function formulation for the RANS simulation of ABL flows. *J. Wind Eng. Ind. Aerodyn.* **2011**, *99* (4), 267.
(40) Hagler, G. S. W.; Lin, M. Y.; Khlystov, A.; Baldauf, R. W.; Isakov, V.; Faircloth, J.; Jackson, L. E. Field investigation of roadside vegetative and structural barrier impact on near-road ultrafine particle concentrations under a variety of wind conditions. *Sci. Total Environ.* **2012**, *419*, 7.
(41) *ANSYS Fluent 12 User's Guide*; ANSYS, Inc.: Lebanon, NH, 2009.
(42) Galeev, A. D.; Salin, A. A.; Ponikarov, S. I. Consequence analysis of aqueous ammonia spill using computational fluid dynamics. *J. Loss Prev. Process Ind.* **2013**, *26* (4), 628.